1977SSRv...21..355S

COSMIC RAY INVESTIGATION FOR THE VOYAGER MISSIONS; ENERGETIC PARTICLE STUDIES IN THE OUTER HELIOSPHERE—AND BEYOND

E. C. STONE and R. E. VOGT*
California Institute of Technology, Pasadena, Calif. 91125, U.S.A.

F. B. McDONALD, B. J. TEEGARDEN and J. H. TRAINOR
Goddard Space Flight Center, Greenbelt, Md. 20771, U. S. A.

J. R. JOKIPII
University of Arizona, Tucson, Ariz. 85721, U. S. A.

and

W. R. WEBBER
University of New Hampshire, Durham, N. H. 03824, U. S. A.

(Received 24 May, 1977)

Abstract. A cosmic-ray detector system (CRS) has been developed for the Voyager mission which will measure the energy spectrum of electrons from ≈3–110 MeV and the energy spectra and elemental composition of all cosmic-ray nuclei from hydrogen through iron over an energy range from ≈1–500 MeV/nuc. Isotopes of hydrogen through sulfur will be resolved from ≈2–75 MeV/nuc. Studies with CRS data will provide information on the energy content, origin and acceleration process, life history, and dynamics of cosmic rays in the galaxy, and contribute to an understanding of the nucleosynthesis of elements in the cosmic-ray sources. Particular emphasis will be placed on low-energy phenomena that are expected to exist in interstellar space and are known to be present in the outer Solar System. This investigation will also add to our understanding of the transport of cosmic rays, Jovian electrons, and low-energy interplanetary particles over an extended region of interplanetary space. A major contribution to these areas of study will be the measurement of three-dimensional streaming patterns of nuclei from H through Fe and electrons over an extended energy range, with a precision that will allow determination of anisotropies down to 1%. The required combination of charge resolution, reliability and redundance has been achieved with systems consisting entirely of solid-state charged-particle detectors.

1. Introduction

Within the outer heliosphere and in nearby interstellar space exists a complex hierarchy of energetic particle populations. Above energies of ≈100 MeV/nuc, the galactic cosmic rays are the dominant component. Between 1 and 100 MeV/nuc occur striking changes in the quiet-time particle composition and spectra that signal a different population which originates either from a nearby interstellar source or perhaps somewhere in the yet unexplored distant regions of the solar system. The particle fluxes in this energy region are frequently augmented by flare-associated,

*Principal Investigator of the Voyager Cosmic Ray Experiment.

Space Science Reviews **21** (1977) 355–376. *All Rights Reserved*
Copyright © 1977 by D. Reidel Publishing Company, Dordrecht–Holland

© Kluwer Academic Publishers • Provided by the NASA Astrophysics Data System

1977SSRv...21..355S

impulsive solar particle events. At the lower energies, the turbulence generated by high-speed solar wind streams interacting with slower moving ones accelerates large numbers of protons and helium nuclei and is a major source of ions in the MeV region. Below about 30 MeV, the electron component in the explored regions of the heliosphere appears to originate mainly from the Jovian magnetosphere. With most of our heliosphere as well as interstellar space still unexplored it is expected that even more new components of the energetic particle population will be identified in the future. It is becoming well established that dynamic, magnetized plasmas of all astrophysical scales are frequently the source of large fluxes of energetic ions and electrons. The composition, energy spectra, temporal and spatial variation and arrival directions of these different components contain information on the location of these plasmas and their dynamics as well as the nature of the medium traversed by the particles. The separation of the different populations and the study of their properties require excellent charge, mass and energy resolution over an extended range of all three parameters. To meet these objectives, an instrument consisting of three basic particle detector systems has been developed for the Voyager mission.

2. Science Objectives

In this section we present a brief overview of what is presently known about the major energetic-particle components, and we discuss the expected impact of the Voyager cosmic ray investigation. In this spirit many of the references are conveniently directed to review papers.

A. Galactic cosmic rays

Of basic importance is the energy density of this component in the galaxy (≈ 1 eV/cm^3), which is of the same order as the energy density of starlight, of interstellar magnetic fields, of the 3° blackbody radiation and of the turbulent motion of interstellar matter. Galactic cosmic rays thus contribute a major element to galactic dynamics.

The cosmic-ray composition and energy spectra are the result of the physical processes connected with their synthesis, their acceleration and their propagation through the interstellar medium. Their composition includes all elements present in the periodic table. For $Z \leqslant 26$, the more abundant elements in cosmic rays are also the more abundant in Solar System matter (Meyer *et al.*, 1974). However, detailed comparisons (Figure 1) show that cosmic rays (referenced to C), are depleted in H, He, and O, and enriched in Mg, Si, Fe and Co. Comparison of the derived cosmic-ray source abundance with the calculations of explosive nucleosynthesis suggests that the particle sources are highly evolved stars with masses greater than 5 solar masses (Meyer *et al.*, 1974).

Another group of elements, d, Li, Be, B, F, K, Sc, Ti, and V, show a relative cosmic ray abundance which is orders of magnitude larger than their solar-system abundance. These elements are produced almost exclusively by spallation of higher-Z

© Kluwer Academic Publishers • Provided by the NASA Astrophysics Data System

1977SSRv...21..355S

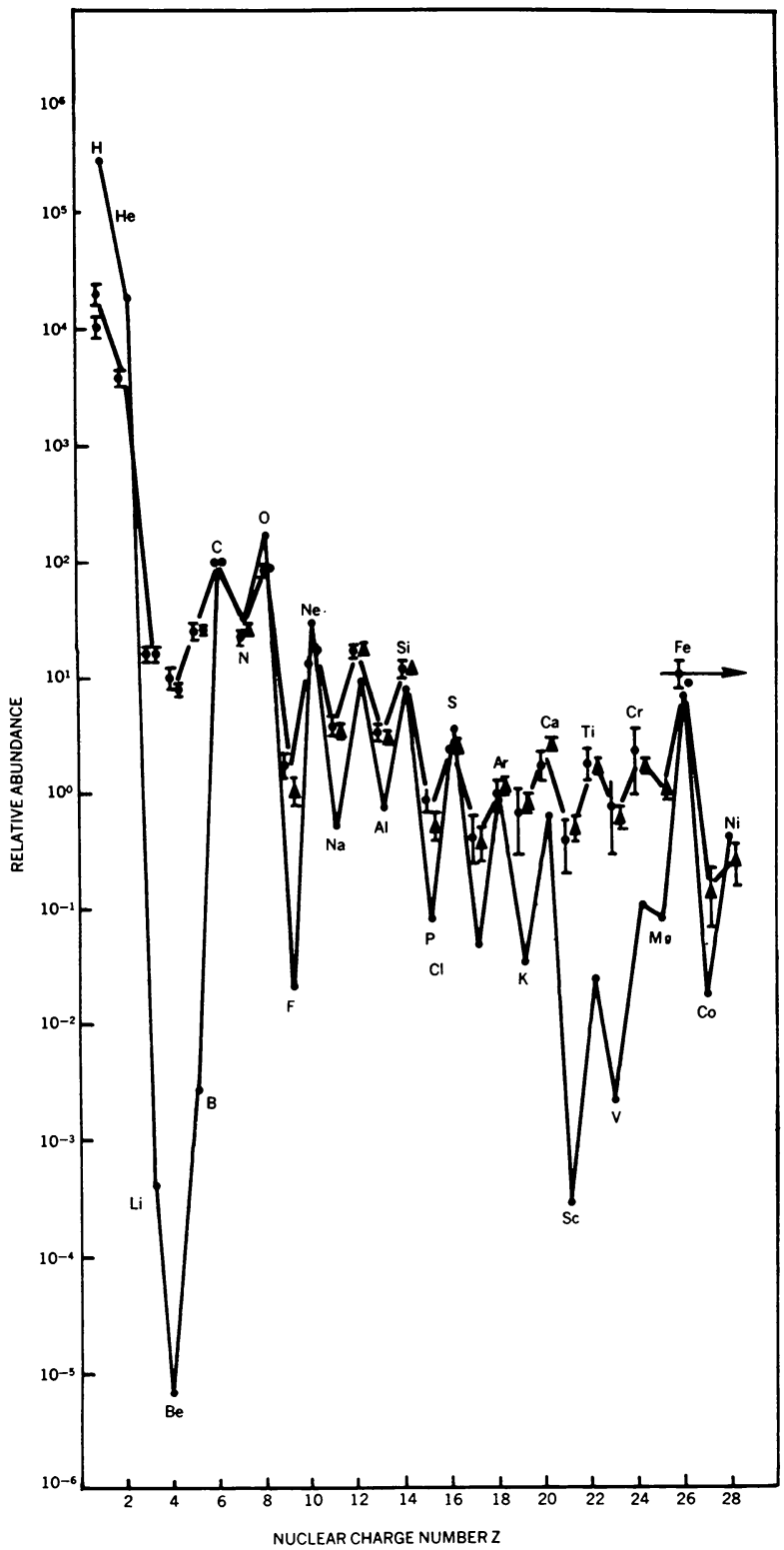

Fig. 1. Relative abundances of the elements from hydrogen to iron, normalized to carbon. The closed circles without error bars which are joined by a light line represent the element abundances in the Solar System. The symbols for the cosmic-ray abundances at 1 AU represent results from different experiments. This experiment will cover the same range of elements with emphasis on particle composition as a function of energy.

© Kluwer Academic Publishers • Provided by the NASA Astrophysics Data System

1977SSRv...21..355S

primaries in the interstellar medium and thus provide information on interstellar propagation. The remaining nuclei for $Z \leqslant 26$ have significant contributions from both cosmic-ray sources and the interstellar spallation of heavier nuclei.

Measurement techniques for low-energy galactic cosmic rays make it possible to obtain information on particle acceleration and interstellar propagation which cannot be achieved at higher energies. For example, isotopes can presently be resolved in the energy range of $\approx$ 1–200 MeV/nuc, and the isotopic composition will provide much more detailed information on the nature of the nucleosynthesis processes in the source region than elemental data alone. Several radio-active isotopes, such as ^{10}B and ^{26}Al, which are mainly interstellar secondaries, make possible a determination of the average lifetime of the cosmic rays in the interstellar medium. Furthermore, ionization energy losses during interstellar propagation should produce systematic changes in the low energy spectra of various nuclear species. In addition this low energy component contains a so far unknown fraction of the total cosmic ray energy.

This energy region which can provide such a wealth of astrophysical information is also the region that is most severely affected by solar modulation. As the cosmic rays penetrate into the heliosphere they encounter magnetic irregularities moving outward in the solar wind. The resulting processes of particle diffusion, convection and adiabatic energy loss in the expanding solar wind result in significant intensity modulation of cosmic rays with energies below 500 MeV/nuc (e.g. Jokipii, 1971, Fisk, 1974). The calculated interplanetary energy losses are so large that it has even been suggested that primary nuclei with energies up to several hundred MeV/nuc outside the heliosphere were unlikely to be observed at 1 AU (Urch and Gleeson, 1972). This general conclusion holds even if one includes gradient and curvature drifts (Jokipii and Levy, 1977) which reduce the energy loss calculated under the Urch and Gleeson model.

With most of the medium and low energy phenomena almost completely obscured by solar modulation, it is of great importance that precise measurements be made in the distant heliosphere near and beyond the outer boundary of the modulation region. The combined mass, charge and energy resolution of the Voyager cosmic ray experiment is generally superior to those instruments which up to this time have been used for measurements at 1 AU. In addition, these measurements cover a far greater range in mass, charge and energy than their precursors on Pioneer 10 and 11, and will extend to greater heliocentric distances at much higher data rates. These new measurements should provide a much more detailed understanding of the interstellar cosmic ray component including its energy content, the effects of energy loss by ionization in the interstellar medium, and its lifetime.

B. Cosmic ray electrons

The cosmic ray electron component consists of both directly accelerated primaries and interstellar secondaries produced by the decay of charged pions which were created in nuclear collisions (e.g. Meyer 1969, Ramaty, 1974). While their intensity

© Kluwer Academic Publishers • Provided by the NASA Astrophysics Data System

1977SSRv...21..355S

at most energies is only a few percent of the corresponding proton intensity, they are of great astrophysical importance. The electrons produce the non-thermal radio emission observed throughout our galaxy and play a yet to be determined role in producing the diffuse X– and γ–ray background emission. Below ≈ 1 GeV the electron spectrum observed at 1 AU is severely distorted by solar modulation. Estimates of the interstellar electron spectrum can be made using the spectral data of the galactic non-thermal radio emission (Webber, 1968; Cummings *et al.*, 1973). However, these radio measurements are primarily useful above $\approx$1MHz, which correspond to a few hundred MeV electron energy in the assumed galactic magnetic fields. Below 1MHz, the low-energy galactic radio spectrum is observed to turn over and decrease (Alexander *et al.*, 1970). It is usually assumed that this depletion is due to free-free absorption by interstellar hydrogen. However, it is also possible that the electron spectrum itself begins to decrease as well at the equivalent energies. Obviously, the correct interpretation of this feature is of major importance in understanding the conditions in the interstellar medium (e.g., the presence of cold gas clouds and the temperature of the intercloud medium) and the origin of these electrons. Depending on their flux levels, these low-energy electrons could play an important role in producing the diffuse X– and γ–ray background in the galactic disk, they could be important to the dynamics of the galactic disk-halo magnetic-field relationship, and they could provide information on the escape of these electrons from known source regions in the galaxy such as the Crab Nebula.

The key objective of the electron investigation is to make precise measurements over an energy range from 3–110 MeV at large radial distances. Because galactic electrons are only a few percent of the nucleon flux, special efforts must be made to suppress background. For this important objective a new and simple electron telescope has been developed. Detailed calibrations at both electron and high energy ion accelerators verify that the energy response and background suppression meet the requirements of the study.

C. The anomalous cosmic ray component

During the present solar minimum, very large variations as functions of energy have been observed in the respective composition and spectra of quiet-time He, N, and O relative to C. (Hovestadt *et al.*, 1973; McDonald *et al.*, 1974). At 1 AU these appear in the form of a flat helium energy spectrum below ≈ 100 MeV/nuc and a sharp increase in the N and O spectra below ≈ 15 MeV/nuc (Figure 2). At about 10 MeV/nuc, oxygen and nitrogen are about 10 times more abundant than carbon whereas the O/C and N/C ratios are of order one in the solar and the higher energy galactic cosmic rays. Recent studies of the radial gradient of low energy helium and oxygen (McDonald *et al.*, 1977; Webber *et al.*, 1977) show that this component is not of solar origin.

The presence of this anomalous component poses significant difficulties for the conventional cosmic ray modulation theory. Two possible solutions have been proposed. Fisk *et al.* (1974) have suggested that the low energy portions of the helium

© Kluwer Academic Publishers • Provided by the NASA Astrophysics Data System

1977SSRv...21..355S

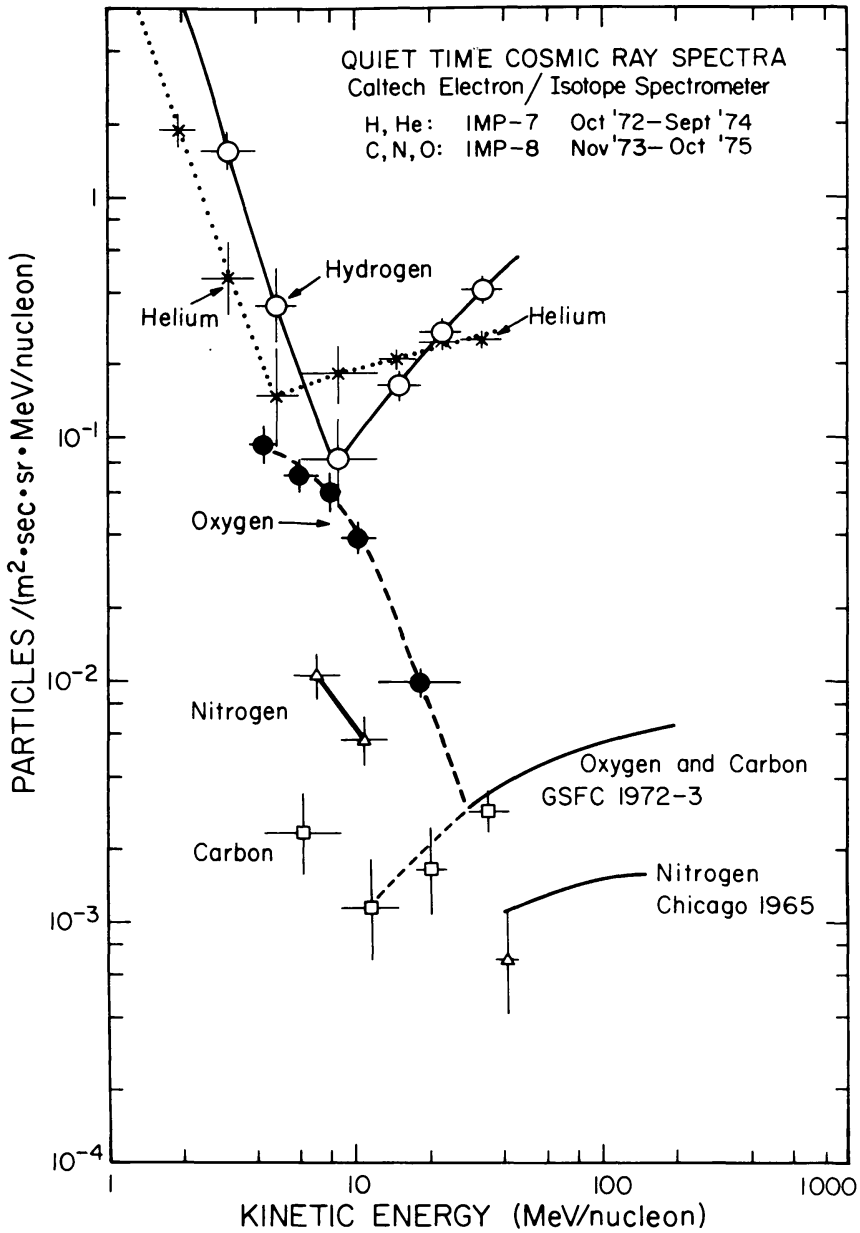

Fig. 2. Typical H, He, C, N and O spectra at 1 AU. Note the flat spectrum of ^{4}He and the anomalous abundances of O and N relative to C between ≈ 2 and 30 MeV/nuc.

and oxygen spectra could result from the flow of neutral, interstellar atoms into the heliosphere. These particles are ionized by both solar ultraviolet and by solar wind particles through charge exchange, and it is postulated that a certain fraction is accelerated by the interplanetary medium. The resulting singly ionized nuclei have much higher rigidities at a given kinetic energy/nucleon and hence, can more effectively penetrate back into the inner heliosphere. An alternate approach is to decrease the commonly assumed residual modulation (by a factor of ≈ 2) of galactic cosmic rays, as, e.g. would be produced by including drift phenomena in modulation theory (Jokipii and Levy, 1977). The average adiabetic energy loss for protons would be lowered from ≈ 300 MeV to ≈ 150 MeV. With this lower value, direct entry of

© Kluwer Academic Publishers • Provided by the NASA Astrophysics Data System

1977SSRv...21..355S

low energy alphas and heavier nuclei into the inner heliosphere becomes possible. In this view the anomalous component is a local interstellar one. Measurements of the isotopic composition by Mewaldt *et al.*, (1976a) have established that the enhanced oxygen and nitrogen fluxes are predominantly ^{16}O and ^{14}N. These values restrict possible nova source models for which the observed nitrogen and oxygen should display enhanced abundances of the ^{15}N and ^{17}O isotopes (Hoyle and Clayton, 1974). The presence of a local interstellar source would not be surprising. Already within the heliosphere there are many different known sources of MeV particles. The inherently larger and more dynamic plasmas outside the heliosphere could be expected to provide a great variety of low and medium energy cosmic ray sources.

It is important that the measurements of anomalous components be extended over a wider charge interval and to lower energies. The effects of possible solar-particle contamination at low energies will be reduced by making these measurements at larger radial distances. Reduced also will be the effects of solar modulation. The ability to resolve isotopes is also of special importance for identifying the origin of this component.

D. Interplanetary acceleration processes

Co-rotating streams of protons, helium nuclei and possible heavier ions are the dominant type of low-energy events observed at 1 AU. They occur in association with high-speed streams in the solar wind and show little correlation with solar flares or radio emission. They typically last for 4–10 days, suggesting widths of 60°–150° at 1 AU. It was originally expected that these co-rotating streams would diminish rapidly with radial distance due both to adiabatic energy loss and spatial effects (Gleeson *et al.*, 1971). However Pioneer 10 and 11 studies (McDonald *et al.*, 1976) have indicated that the intensity of these events frequently increases by a factor of 10–20 out to $\approx$3–4 AU (Figure 3). Helios studies have shown a factor $\approx$10 decrease in intensity between 1 and 0.3 AU. Marshall and Stone (1977) studied the streaming anisotropies of several-MeV protons in these events at 1 AU and found that they were generally streaming in toward the Sun. The energy spectra of the protons are of the form $\exp(-P/P_0)$, where P is the proton momentum and P_0 is generally on the order of $\approx$10–15 MV. The ratio of He/H at a given energy per nucleon usually varies between 0.03 and 0.05. Maximum particle intensities are observed between 2 and 4 AU.

These co-rotating proton events are associated with high speed solar wind streams. Beyond 1 AU the forward regions of these streams steepen into co-rotating shocks (Hundhausen and Gosling, 1977, Smith and Wolfe, 1976). At this time it is not clear whether the particles are energized by the shock or by the associated turbulence. This acceleration mechanism presumably should be one of the simplest ones to study.

It is essential that detailed studies of the charge spectra be carried out at low energies. While it was not known that interplanetary acceleration was an important process when the Voyager proposal was prepared, the characteristics of the cosmic ray experiment are well suited for investigating this new phenomenon. Not only will

© Kluwer Academic Publishers • Provided by the NASA Astrophysics Data System

1977SSRv...21..355S

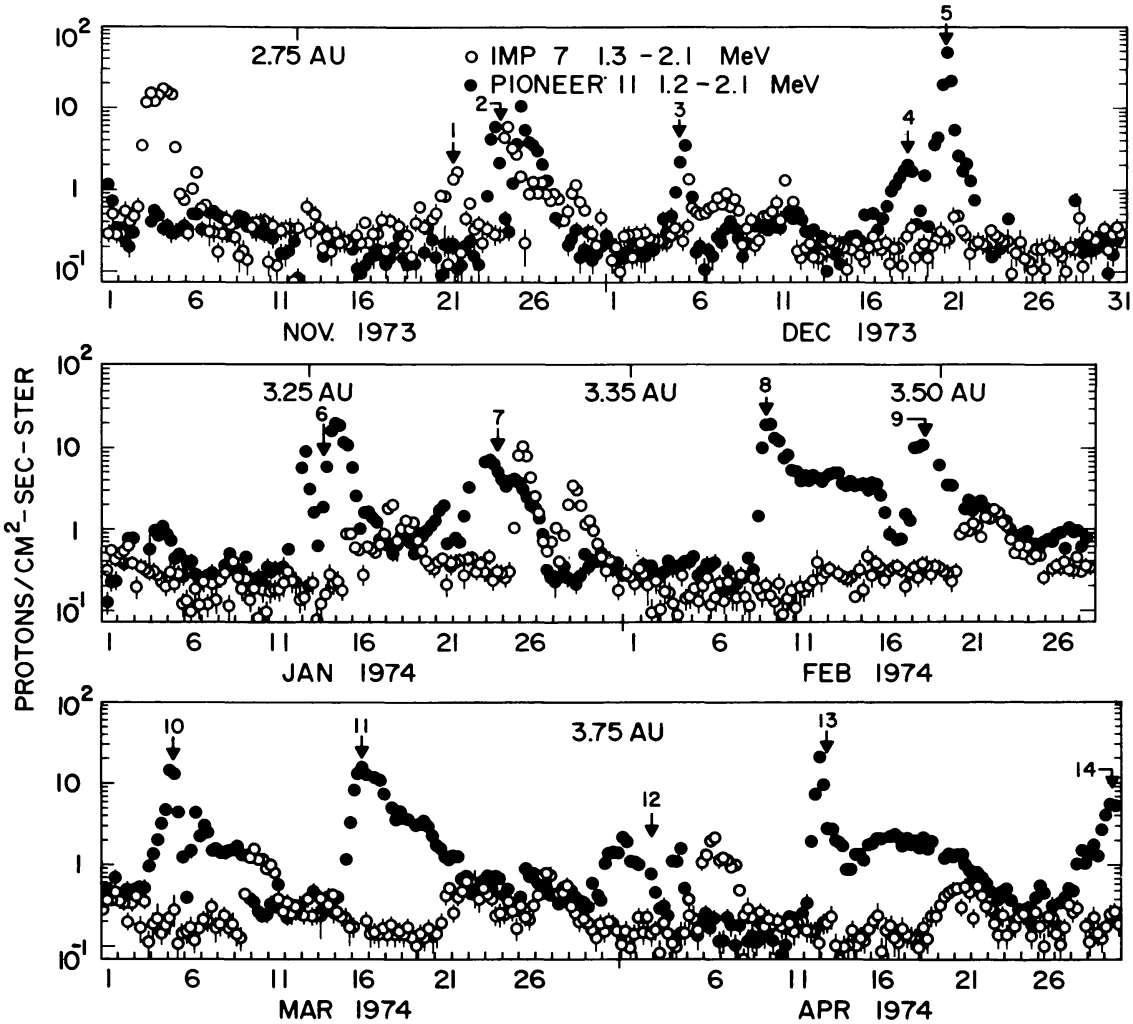

Fig. 3. GSFC IMP-7 and Pioneer-11 flux values for 1.2–2.1 MeV protons for 6-month period extending from 1 November 1973 to 1 May 1974. Data have been averaged over 6-hour periods. The increase in early November appears to be the only flare-associated increase in this period. The co-rotating increases which exceeded 1 proton/cm^2-sec ster-MeV have been numbered. Only one co-rotating event (No. 1) is larger on IMP7 than on Pioneer 11.

it be possible to study the charge and energy spectra, but the low-energy detector system also provides an excellent measurement of the three-dimensional streaming patterns of these particles.

E. Jovian electrons

Below ≈ 40 MeV the electron spectrum observed at 1 AU exhibits a sharp turn-up of the form $\sim T^{-2}$ (where $T =$ kinetic energy). Prior to 1973 it had been observed that this spectral region underwent very unusual time variations, including intensity increases of the order of 200–500%, with durations from 5–12 days, and an anti-correlation with low-energy co-rotating proton events. The intensity variations could not be associated with solar activity, and so it was generally assumed they were galactic. However as Pioneer 10 approached Jupiter both the University of Chicago (Chenette *et al.*, 1974) and Goddard/University of New Hampshire instruments

© Kluwer Academic Publishers • Provided by the NASA Astrophysics Data System

1977SSRv...21..355S

(Teegarden *et al.*, 1974) detected low-energy ($\approx$0.2–8 MeV) electrons from the planet. These electrons occurred in discrete bursts or increases, typically several hundred times the normal quiet-time flux, and becoming much more frequent as one approached Jupiter. Close to Jupiter, but well outside of its magnetosphere, a quasi-continuous presence of large fluxes of these electrons was observed.

Subsequent re-examination of the earlier quiet-time electron data over an 8-year period revealed a striking 13-month periodicity with the maximum increases generally centered about the period when the nominal interplanetary magnetic field connected Earth and Jupiter. Simultaneous observations by Pioneer 11 at 3 AU, IMP 7 at 1 AU and Pioneer 10 at the edge of the Jovian magnetosphere have further confirmed the Jovian magnetosphere as the source of these electrons (McDonald and Trainor, 1976). Further studies over the solar minimum period 1972–1976 (Mewaldt *et al.*, 1976b) have shown that the increases can be detected over an entire year (Figure 4). It now appears most probable that most electrons in the low energy

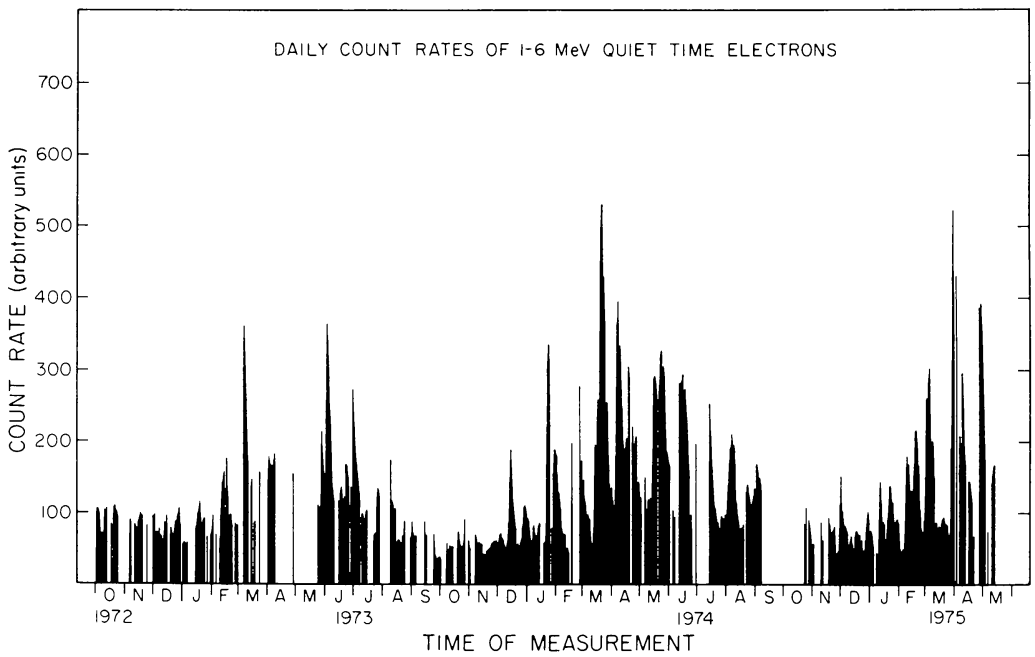

Fig. 4. Jovian electron increases observed at 1 AU with the Caltech IMP 7 and 8 instruments.

spectral turn-up are of Jovian origin. The electron increases have been observed inside 0.4 AU and out to 10 AU. How these ubiquitous particles are transported throughout much of the heliosphere from essentially a point source at 5 AU remains a major problem, the solution of which is bound to provide significant new insight into cosmic ray transport processes.

In the 3–10 MeV electron range the sensitivity of the cosmic ray instrument is significantly greater than that of instruments which have flown at 1 AU so far. It should thus easily be possible to study the properties of Jovian electrons out in the distant heliosphere. In addition, during its passage from Jupiter to Saturn, the

© Kluwer Academic Publishers • Provided by the NASA Astrophysics Data System

1977SSRv...21..355S

Voyager spacecraft will be near the extended Jovian magnetotail, making it possible to determine what role this region plays in the transport of these particles.

F. Arrival direction of low energy cosmic rays

This key observable in cosmic ray physics has yet to be fully exploited, and studies of low-energy flow patterns are a major objective of the Voyager cosmic ray experiment. The complete determination of both the isotropic component and the streaming vector (anisotropy) of the cosmic ray flux over a wide range of energies and elements will greatly aid the analysis of interstellar-particle propagation phenomena. One of the most exciting products of the measurements of cosmic ray anisotropies would be the identification of a specific astrophysical object, e.g., a pulsar or supernova remnant, as the source of an identified component of the observed cosmic ray flux.

Source identification can be attempted from the measurements of the interstellar streaming patterns and the energy spectra of low-energy cosmic rays over an elemental domain ranging from hydrogen through iron, provided the Voyager spacecraft penetrates the modulation boundary. The anisotropies are expected to be most pronounced (in the order of tens of percent) in the low-energy range where pathlength limitations due to heavy ionization losses are most significant, and where the sources therefore must be close. For example, a 1 MeV proton has an integral pathlength $L \leqslant 200$ pc in interstellar gas of $n = 1$ cm^{-3}, and diffusive propagation with a mean freepath $\lambda \approx 30$pc restricts the distance of their source to less than ≈ 100 pc.

It must be noted that the structure of the interstellar diffusive medium will impose its signature on the propagation vector, which thus will tell us something about the features of the galactic magnetic fields, but not necessarily the source direction. Source identification has to be derived from the analysis of a combination of observed parameters. Identification of a source will be aided by the fact that potential sources are extremely rare within the volumes under discussion; e.g. statistically, one expects only a few supernovae remnants in a 10 MeV pathlength source volume, with additional restrictions being imposed by source age. Since ionization losses are governed by the square of the particle's charge (Z^2), consistency checks between anisotropies and energy spectra of elements differing widely in charge ($1 \leqslant Z \leqslant 26$) can be used to separate local origin elements from those at large distances which may have been decelerated to lower energies in their propagation through the galaxy.

G. Other objectives

There are several other study areas where this investigation should make important contributions. The large geometric factors of the detector system will permit detailed study of the dynamics of solar cosmic ray events even to very large radial distances. This study of the interplanetary propagation of particles impulsively injected from the Sun will complement the measurements of the radial variations of galactic cosmic

© Kluwer Academic Publishers • Provided by the NASA Astrophysics Data System

1977SSRv...21..355S

rays. In addition this investigation will yield important information about the magnetospheres of Jupiter and Saturn. On Pioneer 10 and 11 conventional cosmic ray instruments functioned over most of the Jovian outer magnetosphere ($>25R_J$). Pioneer 10 also demonstrated that in this region, the proton anisotropies are a complex mixture of co-rotation, intensity gradients and field aligned flow (McDonald and Trainor, 1976). The Voyager multi-element cosmic ray system is well suited to study these distributions, and in addition, it will be making charge composition measurements at much lower energies than the Pioneer 10 and 11 experiments. These Jovian studies complement those of the Low-Energy Charged-Particle Experiment on the Voyager spacecraft.

3. The Detector Systems

To study the energetic particle phenomena discussed in the previous section a set of three basic detector systems has been developed. The charge, mass and energy intervals covered by these detectors are summarized as follows:

(a) Nuclei charge and energy spectra: $Z = 1$–30, energy range 1–500 MeV for H to 2.5–500 MeV/nuc for Fe.

(b) Isotopes: $Z = 1$–8 ($\Delta M = 1$), energy range 2–75 MeV/nuc

(c) Electrons: 3–110 MeV

(d) Anisotropies: All components ranging from H (1–150 MeV) to Fe (2.7–500 MeV/nuc) as well as 3–10 MeV electrons.

This combination of charge, energy, and mass resolution, reliability and redundancy has been realized with particle telescopes consisting entirely of solid-state charged-particle detectors. These devices have proven to be highly reliable in their space application.

The Voyager cosmic ray detector systems are: the High Energy Telescope System (HETS), the Low Energy Telescope System (LETS), and the Electron Telescope (TET). By using three independent systems, the charge and energy response and the background rejection can be optimized over a given energy interval while providing the redundancy that is vital for an extended mission. By using three-parameter analysis over almost the complete energy range, through the use of curved dE/dx devices to reduce the path-length variations, through choosing the thickest dE/dx device appropriate to a given energy interval to minimize Landau effects, we feel that the ideal solid-state-detector resolution will be approached. The use of two double-ended High Energy Telescopes and the use of multiple (4) Low Energy Telescopes provides the necessary geometric factor to do isotope and charge studies as well as measure low-level anisotropies. These systems have evolved from the GSFC-UNH Pioneer 10 experiment and the CIT IMP-7 and OGO-VI experiments. The flight instrument is shown in Figure 5. In the following section the characteristics of the three different systems are discussed.

© Kluwer Academic Publishers • Provided by the NASA Astrophysics Data System

1977SSRv...21..355S

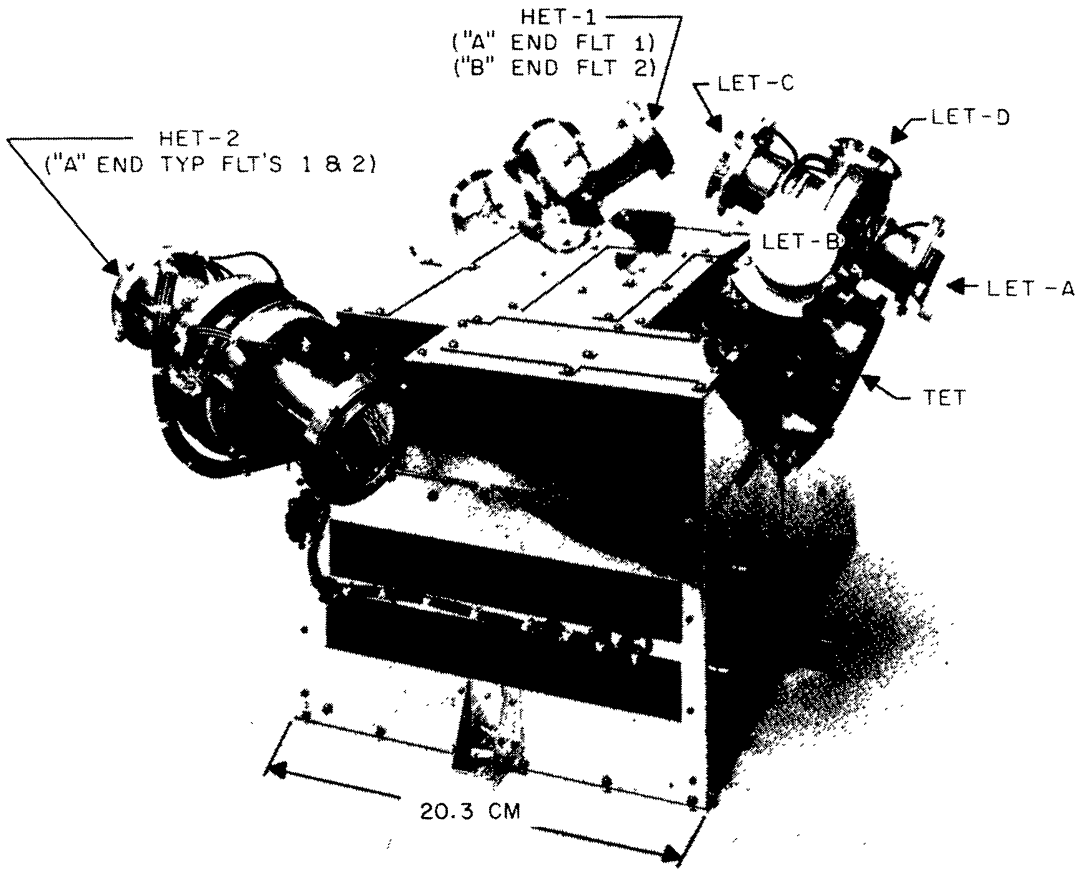

Fig. 5. The assembled Voyager cosmic ray experiment. The weight is 7.5 kg and the nominal power is 5.35 W.

A. The high energy telescope system (HETS)

The system possesses two complete HET telescopes which have nearly orthogonal viewing directions. They have the following characteristics:

(a) The spectra of electrons and all elements from hydrogen to iron will be measured over a broad range of energies.

(b) Individual isotopes can be resolved up through the isotopes of oxygen ($\Delta M = 1$ for $Z = 1$–8); individual charges will be resolved up through $Z = 30$.

Each High Energy Telescope (HET) is double-ended (Figure 6) and has its own associated electronics (Figure 7). A portion of the electronics is also shared with the LET system. The HET telescope is a unique combination of solid-state detectors: A_1 and A_2 are thin surface barrier detectors, B_1 and B_2 are curved Li-drifted detectors, and C_1 through C_4 are the central areas of double-grooved Li-drifted detectors. The combination of a double-ended telescope and the inclusion of a solid-state guard element permits up to a twenty-fold increase in geometry factor over earlier designs. The double grooves create annular detectors around each central area. The annular detectors taken together constitute an anti-coincidence or guard detector (denoted G) surrounding C_1 through C_4. A double-grooved detector is shown in Figure 8.

© Kluwer Academic Publishers • Provided by the NASA Astrophysics Data System

1977SSRv...21..355S

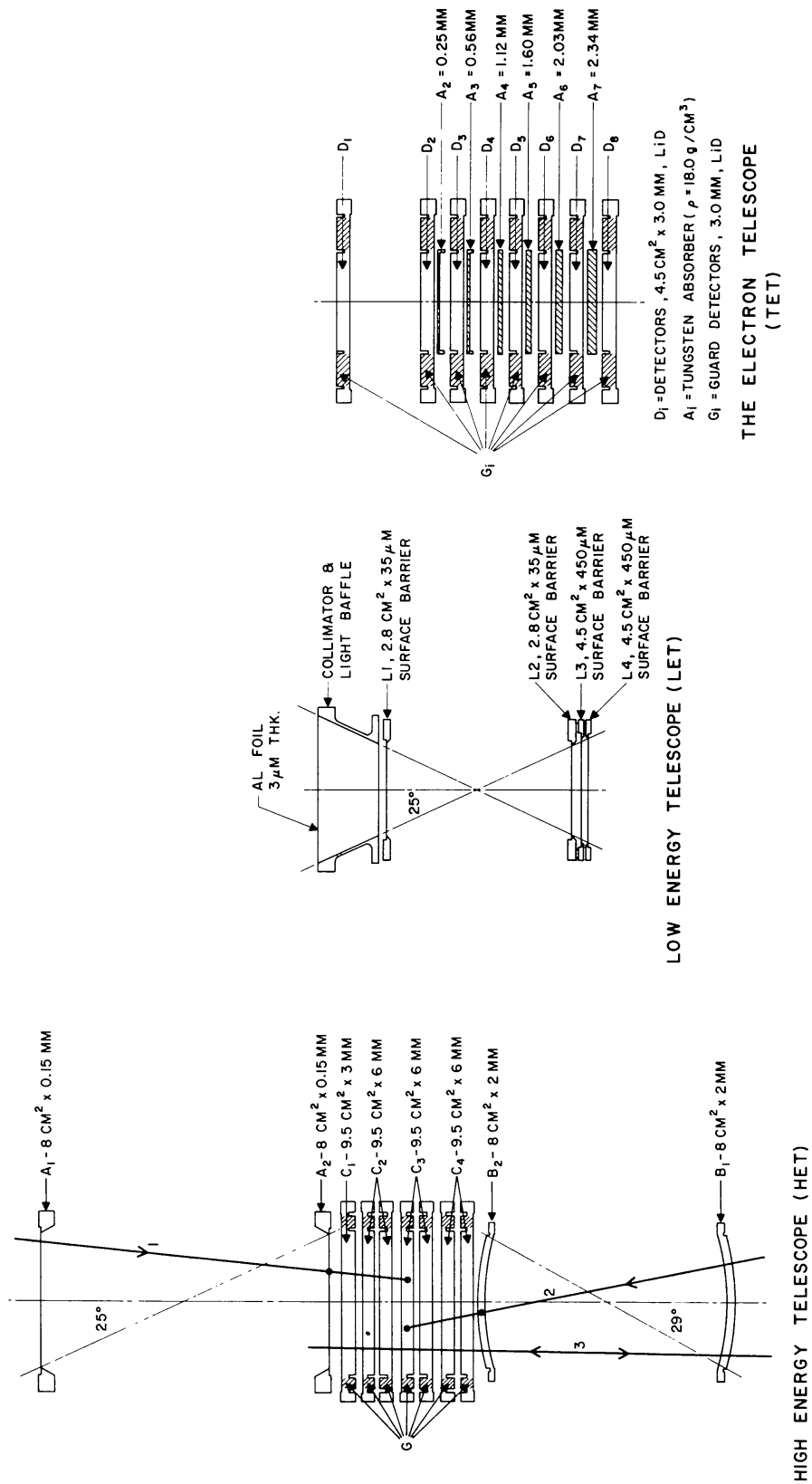

Fig. 6. Schematic of the HET, LET and TET detector systems.

© Kluwer Academic Publishers • Provided by the NASA Astrophysics Data System

1977SSRv...21..355S

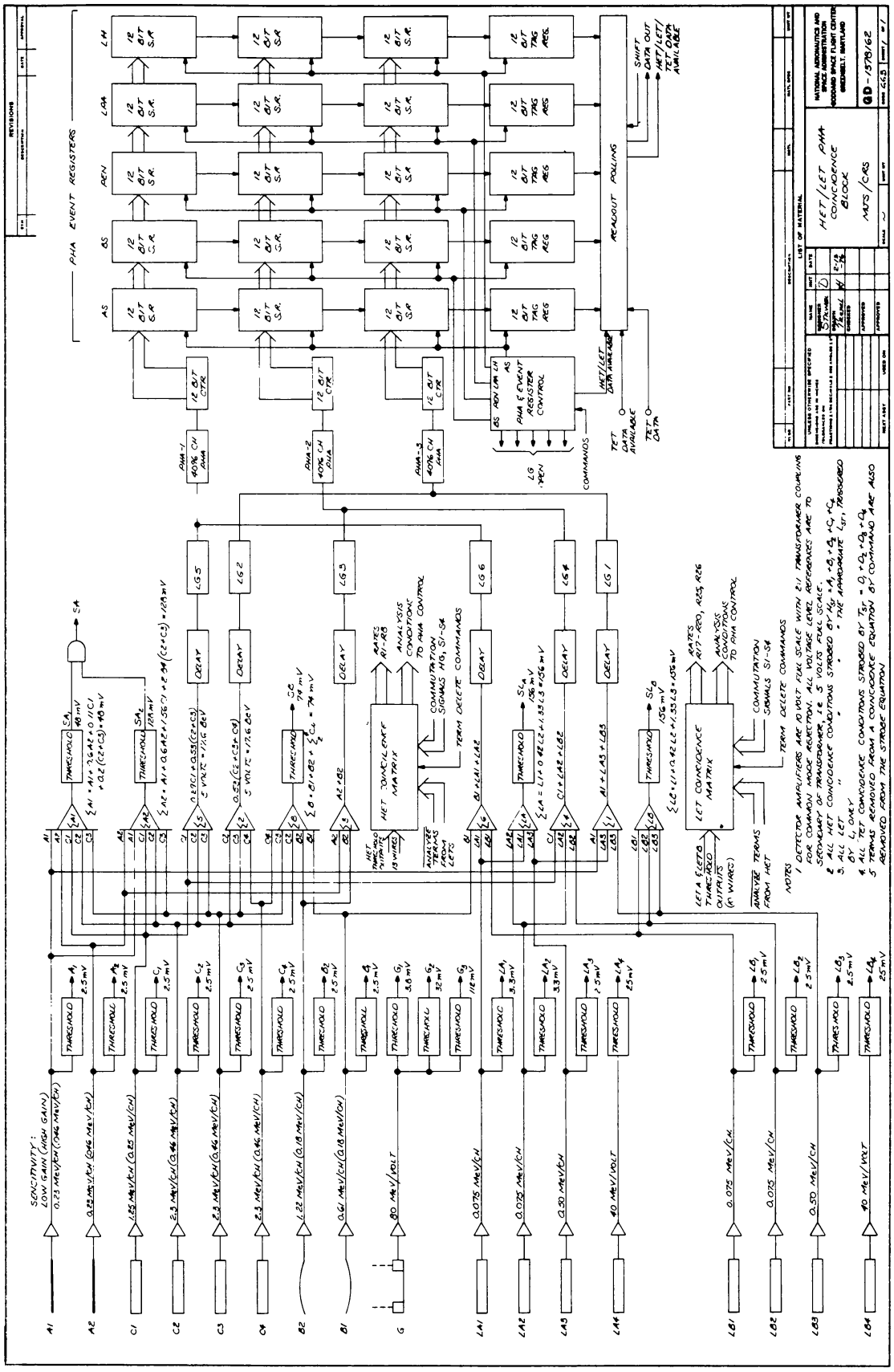

Fig. 7. Diagram of one HET/LET electronic system. There is an identical system for the other HET and 2 LET telescopes. Note that the HET and LET systems share the same post-amplifiers and pulse height analysers. The tag bits identify the telescope where the event originated as well as the event type.

© Kluwer Academic Publishers • Provided by the NASA Astrophysics Data System

1977SSRv...21..355S

Accelerator tests indicate that cross talk between the central and annular areas is less than one part in 2000. The B detectors are curved to minimize variations in particle path length in these detectors due to the finite telescope opening angle.

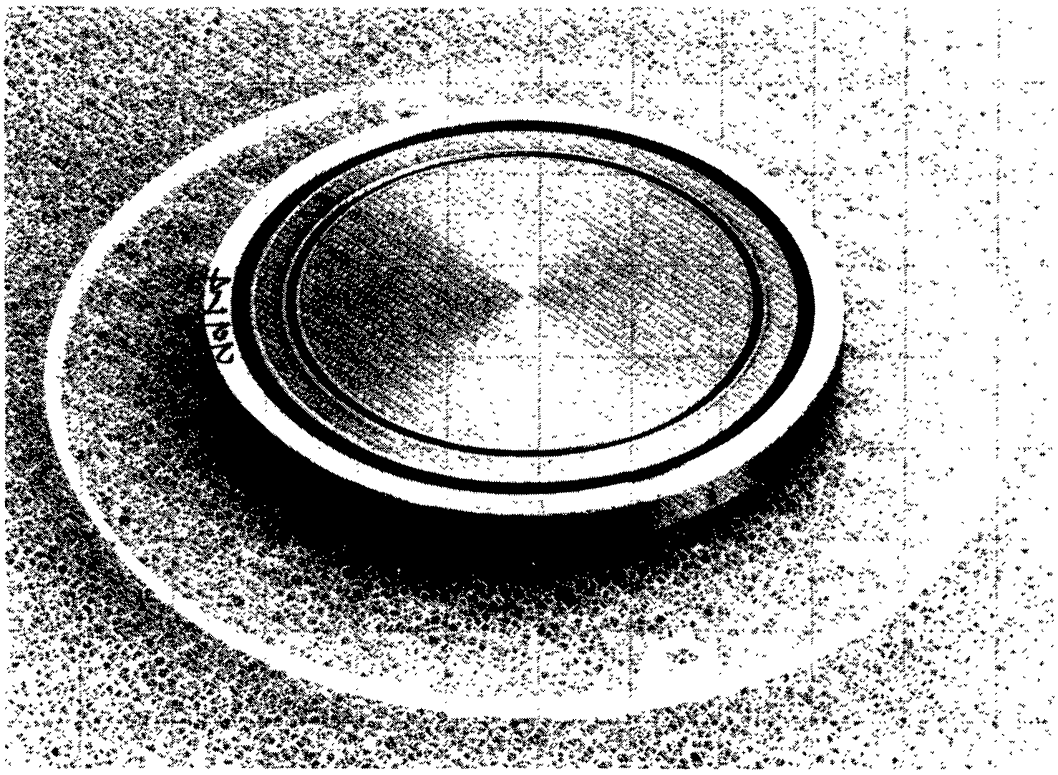

Fig. 8. Picture of double-grooved detector used in the HET telescopes. A similar device with wider guard ring is used in the TET telescope. (The detector is resting on a glass dish.)

Three classes of events are recognized by the electronics, two stopping (S_1 and S_2) and one penetrating (P), as described in Table I.

Event type S_1 represents particles which enter through A_1A_2 and stop in the active volume of the telescope. S_2 events are stopping particles which enter from the B side, and type P events penetrate B_1 and B_2 and the complete C stack.

TABLE I

HET telescope parameters

Event type	Type of analysis	Proton energy range (MeV)	Coincidence condition	Detectors analyzed	Geometry factor (cm^2–ster)	Telescope view angle
S_1	dE/dx vs E	4–57	$A_1A_2\bar{C}_4\bar{G}$	$A_1, A_2, C_1+C_2+C_3$	1.0–1.7	58°
S_2	dE/dx vs E	18–70	$B_1B_2\bar{C}_1\bar{G}$	$B_1, B_2, C_2+C_3+C_4$	0.9–1.7	58°
P	Triple dE/dx	70–500	$B_1B_2C_1$	$B_1, C_1, C_2+C_3+C_4$	1.7	46°

© Kluwer Academic Publishers • Provided by the NASA Astrophysics Data System

1977SSRv...21..355S

In the S_2 mode precise measurements of the electron spectrum in the 3–10 MeV interval will also be made. Below 3 MeV, background due to Compton electrons from the spacecraft radio-isotope power supplies will prohibit quiet-time electron measurements. However, interplanetary electron increases due to solar flares and large events associated with Jupiter will be observable below 3 MeV. Above 3 MeV the 3–10 MeV electron sensitivity should be greater than that of any particle telescopes flown so far at 1 AU.

In order to accommodate the very large ranges in particle charge and energy, effective electronic dynamic ranges of up to 40 000 are required. This requirement is met by using 4096–channel pulse-height analyzers (pha) and preamplifiers with two gain modes differing in gain by factors of 5 or 10. Nuclei with charge $Z>2$ are analyzed in both gain modes. In the low-gain mode, however, protons and alphas do not contribute to S_1 events, electrons and protons are excluded from the S_2 events and protons are excluded from P events. For particles entering a HET telescope from either the A or B end, the experiment electronics forms a pulse sum (such as $B_1+0.5B_2+0.142[C2+C3+C4]$), which when applied to a fixed threshold determines whether the event is due to a particle with $Z<$ or $\geqslant 2$. We refer to such a system as a slant threshold. For particles entering from the B end, there is a slant threshold for both high and low gain modes. For particles entering from the A end, there is a slant threshold operating at low-gain mode only and it defines nuclei with $Z\geqslant 3$ and <3. This slant threshold logic is an integral part of many of the rate equations and also forms the basis for the categorization and storing of pha events for readout.

As shown in the HET block diagram, three 12-bit pulse height analyzers are shared by one HET telescope and two LET telescopes. The instrument has two of these shared pha blocks. They are essentially identical and incorporate considerable cross strapping between the blocks to provide redundancy by command. Each pha block incorporates 8 storage registers, a polling system and block select/readout control.

Each block polling system independently scans sequentially through eight event register positions (e.g., LET-S_1, LET-S_2, TET, HET-S_1, LET-S_1, LET-S_2, HET-S_2, HET-P) until it finds a register with data. It then holds at that position until the event has been read out and then advances to the next position, etc. The block select system sends the read envelope and shift signals to the appropriate block if only one block has data, or it alternates between blocks if both have data. Such a polling system optimizes the efficiency of the experiment data system as well as emphasizes rare events in the data in a predictable way.

Typical examples of the expected charge and mass resolution are presented in Table II. It is shown that isotopes are resolved up through oxygen and that individual charges are easily resolved through iron. Isotopes will not be resolved in the P mode.

Schematic curves illustrating the response of a HET for stopping particles in the $\mathrm{d}E/\mathrm{d}x$ by E mode are shown in Figure 9.

© Kluwer Academic Publishers • Provided by the NASA Astrophysics Data System

1977SSRv...21..355S

TABLE II

HET S_1 resolution

Isotope	Energy (MeV/nucleon)	Charge separation (in units of σ_Z)	Isotope separation (in units of σ_A)
O^{16}	69 (mid-range)	15	2.1
	52 (exit C_1)	17	2.4
Be^{10}	41 (mid-range)	24	2.7
Fe^{56}	131 (mid-range)	6.3	—

B. The Low Energy Telescope System (LETS)

The Low Energy Telescope System (LETS) is designed to determine the three-dimensional flow patterns of interstellar and interplanetary cosmic ray fluxes and to extend high resolution elemental measurements ($1 \leqslant Z \leqslant 30$) down to very low energies. It consists of four Low Energy Telescopes (LET). The LETs have been optimized for the interstellar anisotropy measurements by incorporating large area,

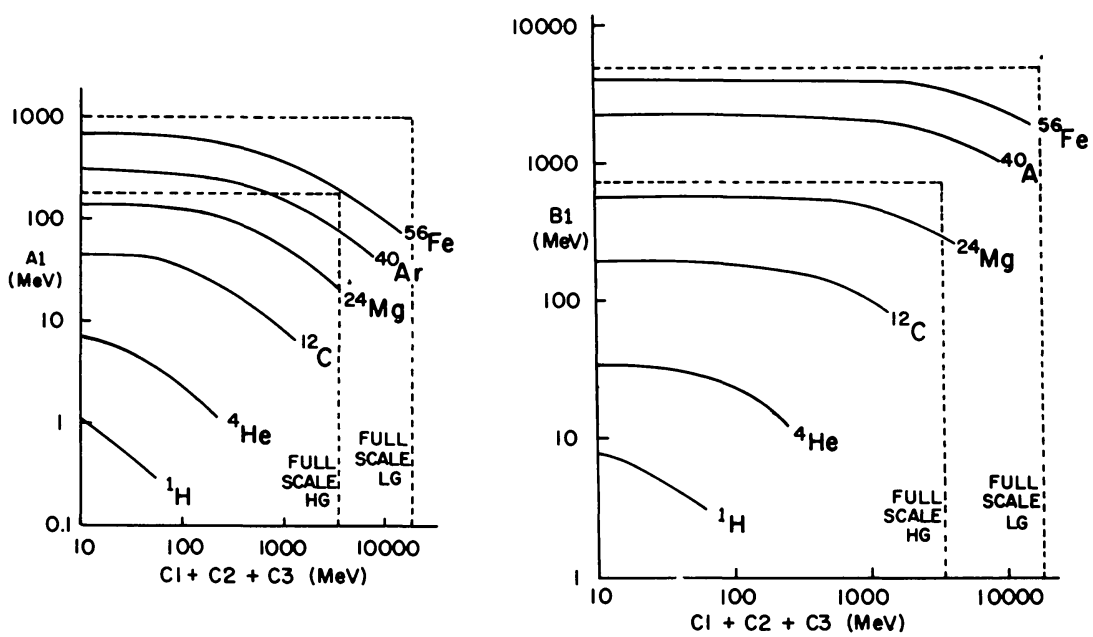

Fig. 9. Calculated HET response curves for stopping particles entering the A and B sides of a HET telescope. Also shown are the limits for the high gain and low gain modes.

© Kluwer Academic Publishers • Provided by the NASA Astrophysics Data System

1977SSRv...21..355S

thin detectors. The LET (Figure 6) provides multi-parameter analysis capability at low energies with the relatively large geometrical factor (0.5 cm^2 sr each) needed for measuring the expected anisotropies. The four LETs are required in order to completely characterize the three-dimensional anisotropy. This arrangement also provides a large total geometrical factor (≈ 2 cm^2 sr), and sensor redundancy.

As shown in the schematic drawing (Figure 6), a 3 μm Al window serves for thermal control and protection from sunlight. All detectors are of the surface barrier type. An important feature is the use of key-hole detectors for $L1$ and $L2$. The active area of the detectors is accurately defined by using a mask to precisely define the area over which the Au and Al contacts are deposited.

Beyond the charge-sensitive preamplifiers and shaping amplifiers, a LET electronics system consists of coincidence circuitry to determine if an event has occurred, pulse-height analyzers and a rate accumulator system as shown previously in Figure 7. As summarized in Table III, there are two analysis modes based upon the amplitude of the sum $L1+0.42\,L2+0.2\,L3$, and events are labeled Type S_1 or Type S_2 accordingly.

TABLE III

LET telescope parameters
(SL = slant condition)

Type	Element	Energy range (MeV/nuc)	Coincidence condition	Detectors analyzed	Geometry factor (cm^2-sr)	Telescope view angle
S_1	$Z \leq 2$	H: 3–8.4	$L1L2L3\overline{L4}\,\overline{SL}$	$L1, L2, L3$	0.44	50°
S_2	$Z \geq 3$	^{16}O:5.3–17	$L1L2L3\overline{L4}\,SL$	$L1, L2, L3$	0.44	50°
		^{56}Fe:7.4–23	$L1L2L3\overline{L4}\,SL$	$L1, L2, L3$	0.44	50°

This is the same type of slant threshold as was discussed for the HET system. However the LET system requires a smaller dynamic range and so gain-switching is not necessary. These events are separately stored and normally read out into telemetry with equal priority in the readout polling scheme. Detector thresholds are set at 200 keV for $L1$ and $L2$, at 1 MeV for $L3$, and at 300 keV for $L4$. Pulse-height analyzers with 4096-channels are provided for $L1$, $L2$ and $L3$. A versatile command system allows for change of the pulse-height analysis conditions, the rate logic, readout priority and power on/off control of the various preamplifiers. E.g., LET analysis may occur also for $L1$ or $L1\,L2$ coincidences. The LET data system and polling were described as part of the HET discussion.

With the specified detector thresholds, the energy ranges specified in Table III are calculated. These calculations are based on the standard energy-loss tables; previous experience shows that corrections to the tables will have to be made on the basis of future calibration data.

Figure 10 shows typical response curves for particles of several types. The energy loss, ΔE, in $L1+L2$ is plotted as a function of residual energy, E', in $L3$. The

© Kluwer Academic Publishers • Provided by the NASA Astrophysics Data System

1977SSRv...21..355S

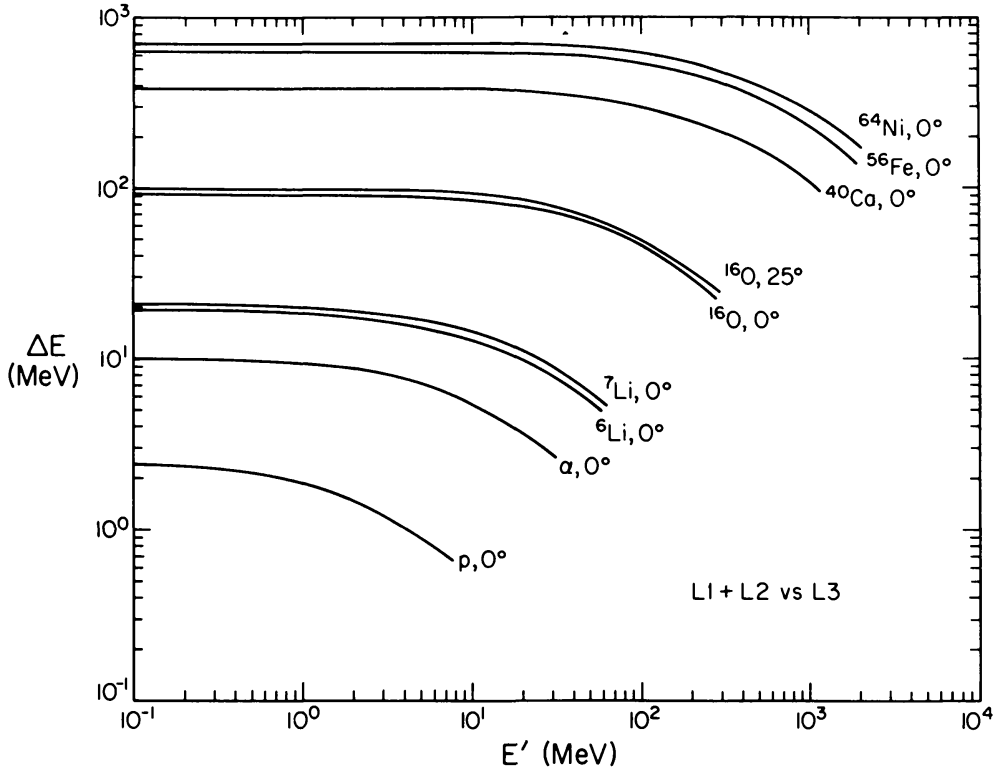

Fig. 10. Calculated LET response for particles which penetrate L_1 and L_2 and stop in L_3. The effects of the finite opening angle are seen for oxygen incident normal to the telescope (0°) and at the maximum opening angle (25°).

different tracks for various particle types can be used to calculate the mass of the particles. Any uncertainties in ΔE or E' result in uncertainties in the calculated mass, with the largest uncertainties being the angle of incidence of the particle.

C. The electron telescope (TET)

A light-weight electron energy-spectrometer has been developed for the energy range from ≈ 5 to 110 MeV. Like the HET, this system uses double-grooved solid state devices which allows an all-solid state detector design with adequate energy resolution and background rejection so that meaningful spectra can be obtained even at the relatively low electron intensities near earth.

Figure 6 gives a schematic cross section of the electron telescope. It consists of eight solid-state detectors (D_1 to D_8) and six tungsten absorbers (A_2 to A_7) in a cylindrical geometry. Like the HET system, the detector-absorber stack is surrounded by a grid of solid-state-guard detectors (G_2 to G_8). The TET electronics are a simplified version of the HET/LET system shown in Figure 7.

Electrons and their energies are identified by a double-dE/dx measurement in detectors D_1 and D_2 and by a simultaneous measurement of their range, as determined by the penetration of detectors D_3 through D_7. The use of range

© Kluwer Academic Publishers • Provided by the NASA Astrophysics Data System

1977SSRv...21..355S

spectroscopy, while providing satisfactory energy resolution and background rejection, has the additional virtue of being insensitive to electronic gain drifts, thus permitting the use of simpler electronics systems.

Energy calibrations of prototypes of electron range-telescopes for energies from 1 MeV to 1 GeV have been performed on particle accelerators (Figure 11). These data allow the unfolding of energy spectra from measured range distributions. As an example, we show in Table IV the expected range distributions (determined from the calibrated detector response) for the three hypothetical electron energy spectra

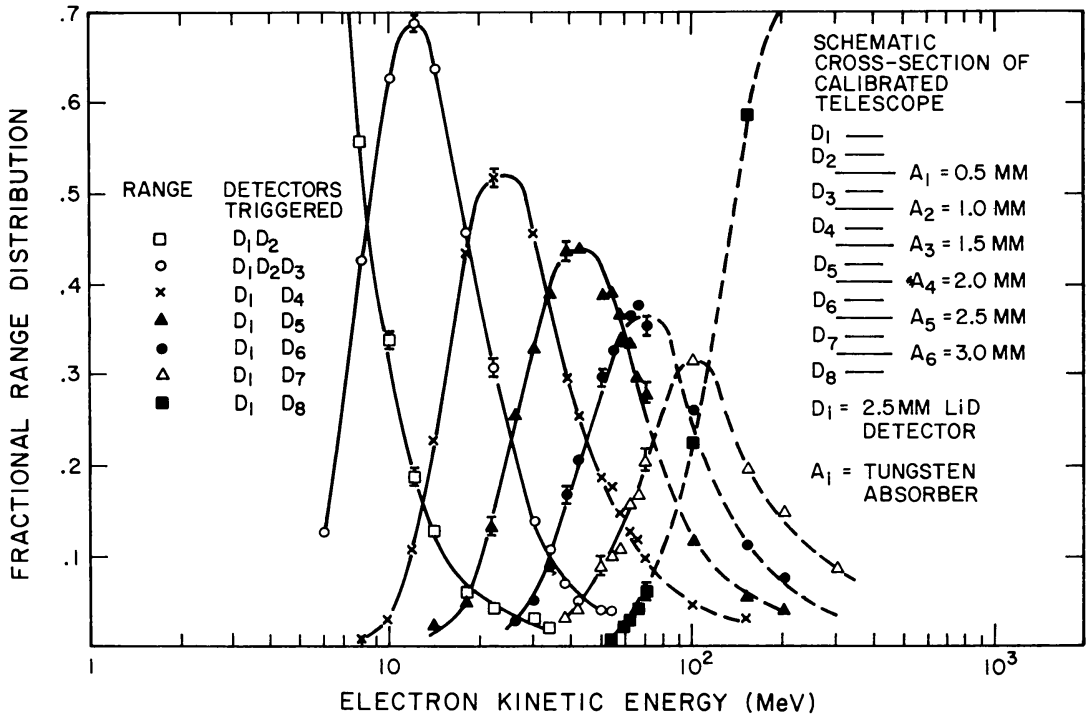

Fig. 11. Electron-calibration results for prototype TET shown in insert. The response curves shown represent the fractional distribution of mono-energetic electrons over the telescope ranges.

shown in Figure 12. The application of a simple unfolding technique to these data results in the very satisfactory reproduction of the input spectra shown by the TET data points in Figure 12. At low energies, the expected data points from the HET telescopes are also included in the figure showing the adequate overlap of energy ranges for TET and HET.

Conservative estimates of maximum background levels during the mission are shown by the dashed areas. This background is generated by the spacecraft Radioisotope Thermal Generators (RTG) (below ≈ 2.5 MeV) and by interacting high-energy protons in the detector stack.

© Kluwer Academic Publishers • Provided by the NASA Astrophysics Data System

1977SSRv...21..355S

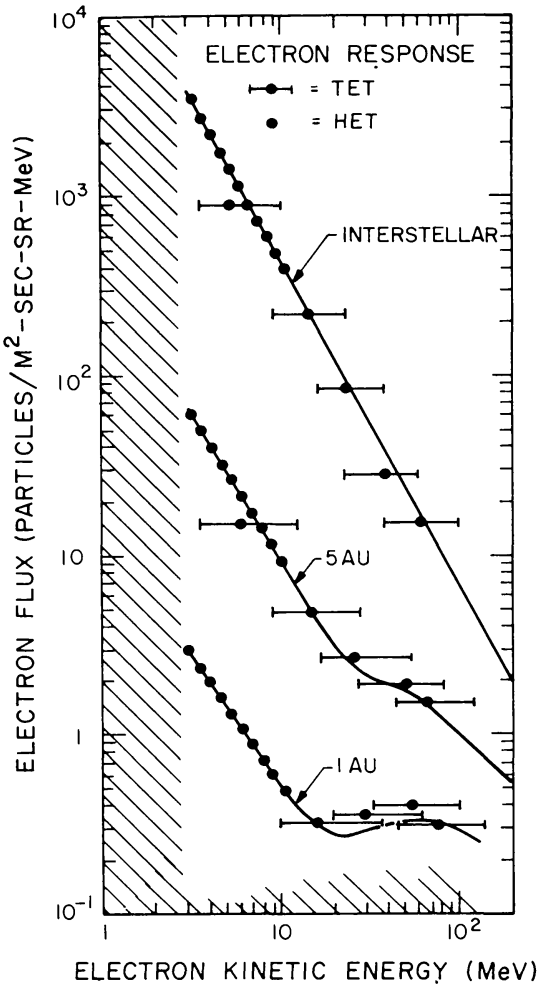

Fig. 12. Hypothetical electron spectra (solid lines) for heliocentric radii of 1 AU, 5 AU and the interstellar medium. Data points show the resolving power of the HET and TET. The dashed area shows the expected RTG and cosmic-ray generated background. The sharp increase in detector background at low energies is due to the RTG.

TABLE IV

TET telescope range distributions and maximum background levels for the three hypothetical cosmic ray electron spectra shown in Figure 12.

Range (D_i's triggered)	Geometry factor (cm^2 sr)	*Counts/Month* 1 AU	5 AU	Interstellar	Max. background
$D_1D_2D_3$	1.8	1.8×10^3	3.4×10^4	1.6×10^6	3.9×10^2
$D_1\ldots D_4$	1.4	1.6×10^3	1.6×10^4	5.2×10^5	5.2×10^2
$D_1\ldots D_5$	1.0	1.4×10^3	8.6×10^3	1.7×10^5	5.2×10^2
$D_1\ldots D_6$	0.8	1.4×10^3	6.0×10^3	7.3×10^4	5.2×10^2
$D_1\ldots D_7$	0.6	1.4×10^3	4.9×10^3	4.2×10^4	7.8×10^2

© Kluwer Academic Publishers • Provided by the NASA Astrophysics Data System

1977SSRv...21..355S

Acknowledgements

The Voyager cosmic ray experimenters would like to acknowledge their gratitude to Donald E. Stilwell, the Experiment Engineer, and to William Althouse, A. C. Cummings, and T. L. Garrard of Caltech; M. F. Beazley, W. D. Davis and H. E. Trexel of Goddard and J. Otte of JPL and the many others whose devotion and hard work made it possible to deliver an experiment whose inflight performance is expected to reach the scientific objectives as originally proposed.

References

Alexander, J. K., Brown, L. W., Clark, T. A., Stone, R. G., and Weber, R. R.: 1969, *Astrophys. J. Lett.* **157**, L163.

Chenette, D. L., Conlon, T. F., and Simpson, J. A.: 1974, *J. Geophys. Res.* **79**, 3551.

Cummings, A. C., Stone, E. C., and Vogt, R. E.: 1973, *Proc. 13th Intl. Cosmic Ray Conf., Denver*, **1**, 335.

Fisk, L. A.: 1974, in *High Energy Particles and Quanta in Astrophysics*, F. B. McDonald and C. E. Fichtel (eds.), M.I.T. Press, Cambridge, p. 170.

Fisk, L. A., Kozlovsky, B., and Ramaty, R.: 1974, *Astrophys. J. Lett.* **190**, L35.

Gleeson, L. J., Krimigis, S. M., and Axford, W. I.: 1971, *J. Geophys. Res.* **76**, 2228.

Hovestadt, D., Vollmer, O., Gloeckler, G., and Fan, C. Y.: 1973, *Phys. Rev. Lett.* **31**, 650.

Hoyle, F. and Clayton, D. D.: 1974, *Astrophys. J.* **191**, 705.

Hundhausen, A. J. and Gosling, J. T.: 1976, *J. Geophys. Res.* **81**, 1436.

Jokipii, J. R.: 1971, *Rev. Geophys. Space Phys.* **9**, 27.

Jokipii, J. R. and Levy, E. H.: 1977, *Astrophys. J.* (in press).

Marshall, F. E. and Stone, E. C.: 1977, *Geophys. Res. Lett.* **4**, 57.

McDonald, F. B., Teegarden, B. J., Trainor, J. H., and Webber, W, R.: 1974, *Astrophys. J. Lett.* **187**, L105.

McDonald, F. B. and Trainor, J. H.: 1976 in T. Gehrels (ed.), *Jupiter*, Univ. of Arizona Press, p. 961.

McDonald, F. B., Teegarden, B. J., Trainor, J. H., von Rosenvinge, T. T., and Webber, W. R.: 1976 *Astrophys. J. Lett.* **203**, L149.

McDonald, F. B., Lal, N., Trainor, J. H., and Van Hollebeke, M. A. I.: 1977, *Astrophys. J.* (in press).

Mewaldt, R. A., Stone, E. C., Vidor, S. B., and Vogt, R. E.: 1976a, *Astrophys. J.* **205**, 931.

Mewaldt, R. A., Stone, E. C., and Vogt, R. E.: 1976b, *J. Geophys. Res.* **81**, 2397.

Meyer, P.: 1969, *Ann. Rev. Astron. Astrophys.* **7**, 1.

Meyer, P., Ramaty, R., and Webber, W. R.: 1974, *Physics Today*, **27**, 23.

Ramaty, R.: 1974, in F. B. McDonald and C. E. Fichtel (eds.), *High Energy Particles and Quanta in Astrophysics*, M.I.T. Press, Cambridge, p. 122.

Smith, E. J. and Wolfe, J. H.: 1976, *Geophys. Res. Lett.* **3**, 137.

Teegarden, B. J., McDonald, F. B., Trainor, J. H., Webber, W. R., and Roelof, E.: 1974, *J. Geophys. Res.* **79**, 3615.

Urch, I. H. and Gleeson, L. J.: 1972, *Astrophys. Space Sci.* **16**, 55.

Webber, W. R.: 1968, *Australian J. Phys.* **21**, 845.

Webber, W. R., McDonald, F. B., Trainor, J. H., and von Rosenvinge, T. T.: 1977, private communication.

© Kluwer Academic Publishers • Provided by the NASA Astrophysics Data System